

Size Analyses and Geochemistry of Ferromanganese Nodules from the Central Indian Ocean Basin

A. B. VALSANGKAR
N. H. KHADGE

National Institute of Oceanography
Dona-Paula, Goa, India, 403 004

Abstract Ferromanganese nodules collected during the 13th cruise of the M. V. Skandi Surveyor in 1987 cover a very large area, 71 424 km² in the Central Indian Ocean. The area consists of 13 nodule types, which are grouped into six size classes. Morphology indicates that spheroidal and ellipsoidal nodules of rough type (Sr) belonging to classes 1 (<2 cm) and 2 (2–4 cm) are more abundant. The concentration of Mn, Fe, Cu, Ni, and Co in 84 samples varies inversely with size class and only class 1 and 2 nodules are found to be enriched in Mn, Cu, Ni, and Co. Excellent correlations are observed between Mn with Cu and Ni and Fe with Co, whereas Mn and Fe behave inversely in all the size classes. The estimated growth rates are inversely related to size and suggest that the smaller nodules of classes 1 and 2 grow rapidly because of an additional source of the transitional elements. Mineralogy of 36 different size nodules shows decreasing abundance of todorokite with increase in size. Systematic compositional variation observed between the six nodule classes is related to the morphology, mineralogy, and contribution of biogenic matter. The nodules of classes 1 and 2 have a higher grade (>2.47% of Cu + Ni + Co) and a higher percentage of abundance relative to the nodules of other classes. The study also implies the importance of selection of size parameter when designing the nodule collector.

Keywords Size, morphology, geochemistry, nodules, XRD, CIOB.

Introduction

Bulk chemistry is one of the important variable parameters of ferromanganese nodules. Previous regional studies on deep-sea nodules are based on bulk chemical composition and many workers have attempted to establish a relationship between composition and basinal characteristics. Mero (1965) first studied the compositional variations in Pacific Ocean nodules. Later, Cronan and Tooms (1969), Price and Calvert (1970), and Piper and Williamson (1977) found their relationship with different marine sedimentary environments. Barnes (1967) and Calvert et al. (1978) discussed elemental and mineralogical variations. Recent investigations on Pacific nodule deposits showed that the nodule characteristics are variable within small areas of undulating topography (Mizuno and Moritani 1978, Andrews and Friedrich 1979, Halbach and Öskara 1979). Heye (1979) and Friedrich et al. (1983) observed some relationship between composition and nodule diameter. In the Central Indian Ocean the regional studies for resource assessment were carried out by Frazer and Wilson (1980), Cronan and Moorby (1981), and Siddiquie et al. (1984).

In this study, the morphological, mineralogical, and geochemical characteristics of the nodules from 36 dredge stations in the Central Indian Ocean Basin (CIOB) are described and their mode of formation is discussed. The metal source of nodules with

respect to the morphology, abundance, and composition is ascertained. An attempt has also been made to ascertain the relationships between nodule mineralogy and the size of the nodules. The growth rates estimated are compared with morphological variations.

Methods

Bottom sampling in the CIOB was carried out using a conventional dredge design during the 13th cruise of the *M. V. Skandi Surveyor*. The dredging operations resulted in bulk collection of nodules of varying morphology. Sometimes, the dredge haul material recovered included fragments of manganese-coated rocks such as pumice and basalt and consolidated pelagic and siliceous sediments. The large quantity of nodules recovered were sorted on board for each dredge haul by passing them through various sieves.

Nodules were classified and their morphology was described following Moritani et al. (1977). The selected nodules were measured for both minimum and maximum diameter, and their weights and composition were compared. Each nodule was cut into two halves. One part was kept for ore microscopic and scanning electron microscopic studies (the results will be presented elsewhere); the geochemical studies were carried out on the remaining half of the selected samples.

With a size difference of 2 cm, six nodule size classes were adopted:

Class No.	Nodule size range (cm)
1	<2.0
2	2.0–4.0
3	4.0–6.0
4	6.0–8.0
5	8.0–10.0
6	>10

Analytical Techniques

A representative nodule from each size class at each dredge haul was chemically analyzed. Bulk chemistry and X-ray diffraction (XRD) analyses of the nodules were carried out for the same samples of each dredge haul. Sample solutions were made by dissolving 0.1 g of sample by open digestion with concentrated HCl–HF–HClO₄ in a Teflon beaker, and the final solutions were made by adding 10 mL of 1:1 HCl. Duplicate samples were analyzed for Mn, Fe, Cu, Ni, and Co by atomic absorption spectrophotometry (AAS) using a Perkin-Elmer model 5000 double-beam spectrophotometer. The NIO standard 2388 was used as an internal standard to confirm the analytical results. Mineralogical identification was carried out by Phillips X-ray diffractometer system with a CuK α radiation and scintillation detector. Growth rates were estimated using the formula by Lyle (1982).

Results

Size Analyses

The water depth in the area ranged from 5025 to 5500 m and the dredging was carried out at 24 stations. Of 36 dredge operations, 7 were carried out at the 15' to 30' interval

on 76°E longitude and similarly 2 on 77°E, 3 on 79°E, and 5 on 79°30'E longitude (Figure 1).

Modal percentage for individual dredge haul at each sampling station is given in Figure 2. From the histograms it is clear that the occurrence of nodules of <4 cm size varies from 50 to 98%, whereas that of 4- to 6-cm-size nodules varies from 1 to 51%; nodules of >6 cm are uncommon. The figure also indicates that at any given dredge haul, the nodules of classes 1 and 2 dominate over the other classes.

Morphology

Nodules of both rough (Sr) and smooth (Ss) surface texture were recovered. However, the smooth nodules are less abundant than the rough nodules (Table 1). Based on the morphological variations, 13 types of nodules were identified. In fact, the majority of class 1 nodules are of the Sr (spheroidal, rough) type and those of class 2 are of the Sr and SPr (spheroidal, intergrown, and rough) type. Class 3 nodules have maximum population of mixed types which include smooth and rough surface texture but DBr (discoidal, botryoidal, and rough) and SEr (spheroidal/ellipsoidal, and rough) nodules dominate. In other classes (4-6), SEr and DBr nodules are more common.

Mineralogy

XRD studies on 36 bulk samples showed interesting results. Using the terminology of Burns et al. (1975), todorokite, birnessite, and δ -MnO₂ are recognized on the basis of diffraction peaks at 9.61 Å, 7.31-6.97 Å, and 2.45-2.40 Å. Quartz and plagioclase dominate among the accessory minerals.

Todorokite occurs as a principal manganese oxide phase in all the samples. The intense and strong peak of todorokite is common in smaller nodules (classes 1-3), whereas

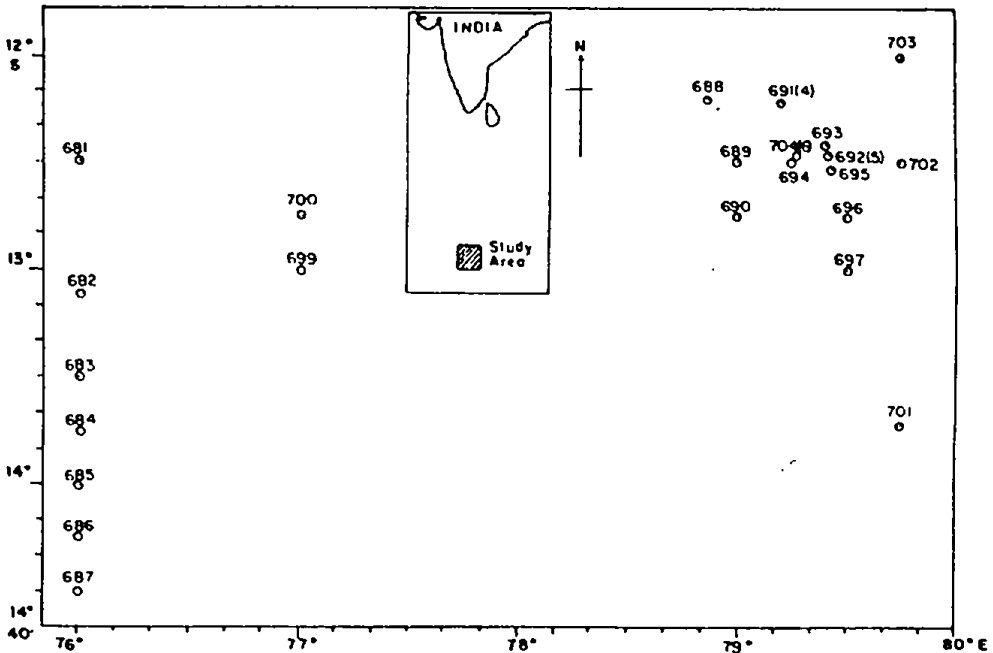


Figure 1. Map showing location of dredge stations in the Central Indian Ocean Basin.

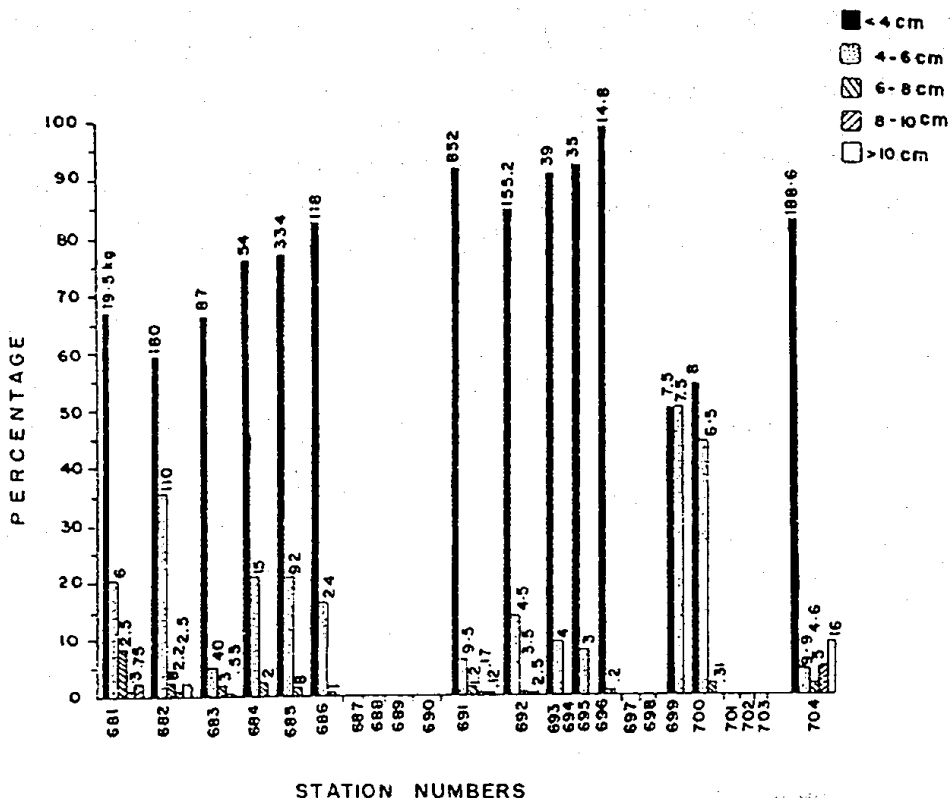


Figure 2. Histograms showing size analyses and abundance percentage of dredge samples from the SS-13 cruise.

intensity and peak height decrease in the nodules of higher classes (5 and 6; Figure 3). Birnessite occurs along with todorokite and behaves similarly, whereas the occurrence of $\delta\text{-MnO}_2$ is independent. The association of these minerals is further reflected in the chemical composition.

Typical XRD patterns of todorokite occurrence are shown in Figure 3. The low and broad peaks indicate low abundance and poor crystallinity. The crystallinity of todorokite typically decreases with an increase in nodule size.

Bulk Chemical Composition

Major element concentrations of 84 samples from 24 different stations are presented on dry basis in Table 1. The table also includes Mn/Fe ratios and growth rates. The growth rates vary from 6 to 20 mm/ma and (Cu + Ni + Co) varies from 0.8 to 3.7%. The ranges (Table 2) and averages (Table 3) display a marked variation in the transition elements. The average bulk composition shows the following ranges: Mn, 16.4–32.8%; Fe, 4.2–16.6%; Cu, 0.3–1.6%; Ni, 0.4–1.4%; Co, 0.1–0.2%; and the moisture content from 6.7 to 20.2%. The average values obtained for all classes are quite similar to those from the average Pacific Ocean nodules (Table 3).

There are four different sets of samples in Table 1 (Sr. Nos. 1–6, 7–12, 13–18, and 71–76) from four stations (681, 682, 683, and 701, respectively), which have all six size classes. Three other sets (Sr. Nos. 31–35, 41–45, and 77–81) have two smaller and one higher class, whereas the rest of the sets have 2–4 lower nodule size classes. In all

Table 1
Bulk Chemical Composition of Nodules from the Central Indian Ocean Basin

Sr. No.	Station No.	Size (cm)	Nodule type ^a	Moisture (%)	Mn (%)	Fe (%)	Cu (%)	Ni (%)	Co (%)	(Cu + Ni + Co) (%)	Mn/Fe	Growth rate (mm/ma)
1	681	<2	Sr	12.90	30.25	6.50	1.55	1.27	0.11	2.92	4.65	11.90
2	681	2-4	Sr	14.93	30.82	6.14	1.58	1.35	0.10	3.04	5.02	13.54
3	681	4-6	SEr	16.21	29.73	6.93	1.44	1.29	0.09	2.82	4.29	10.34
4	681	6-8	DBr	18.59	24.37	7.68	0.98	0.93	0.10	2.01	3.17	7.06
5	681	8-10	Vr	19.66	17.02	7.87	0.57	0.56	0.08	1.21	2.16	4.84
6	681	>10	Sr	17.33	22.79	7.38	0.89	0.84	0.11	1.83	3.08	7.14
7	682	<2	Sr	9.31	22.16	6.41	1.41	1.22	0.12	2.75	3.46	9.09
8	682	2-4	SPr	11.79	28.98	7.09	1.28	1.11	0.11	2.50	4.09	9.69
9	682	4-6	DBr	10.19	28.54	9.17	1.14	1.01	0.15	2.29	3.11	5.88
10	682	6-8	SEr	8.46	27.11	7.47	1.24	1.05	0.11	2.40	3.63	8.22
11	682	8-10	SEr	13.52	25.29	10.41	0.89	0.86	0.14	1.89	2.43	4.18
12	682	>10	IBr	13.77	23.51	9.72	0.79	0.74	0.14	1.67	2.42	4.43
13	683	<2	Sr	14.81	30.71	6.04	1.53	1.26	0.10	2.89	5.08	13.91
14	683	2-4	SPr	11.61	28.78	6.32	1.37	1.13	0.11	2.61	4.55	11.97
15	683	4-6	SPr	10.97	28.47	6.69	1.37	1.17	0.10	2.65	4.26	10.63
16	683	6-8	DBr	15.77	28.16	7.68	1.22	1.10	0.12	2.44	3.67	8.08
17	683	>10	DBr	20.21	21.73	8.66	0.71	0.76	0.11	1.62	2.51	5.08
18	684	<2	SPr	16.30	31.89	8.79	1.32	1.08	0.11	2.71	3.63	7.06
19	684	2-4	SPr	13.96	29.42	7.09	1.25	1.06	0.12	2.42	4.15	9.81
20	684	4-6	SEr	15.98	27.22	9.36	1.03	0.89	0.13	2.05	2.91	5.42
21	684	6-8	SEr	15.40	27.37	8.17	1.07	0.93	0.11	2.11	3.35	7.01
22	685	<2	Ss/SPs	10.51	29.06	7.97	1.16	1.08	0.15	2.39	3.65	7.77
23	685	2-4	IDPs	13.97	24.51	13.16	0.65	0.65	0.18	1.47	1.86	2.71

(Table continues on next page)

Table 1 (continued)

Sr. No.	Station No.	Size (cm)	Nodule type ^a	Moisture (%)	Mn (%)	Fe (%)	Cu (%)	Ni (%)	Co (%)	(Cu + Ni + Co) (%)	Mn/Fe	Growth rate (mm/ma)
24	685	4-6	Ss/SPg	14.38	26.68	10.13	0.95	0.90	0.14	1.99	2.63	4.61
25	685	6-8	IBr	14.68	23.22	13.96	0.55	0.57	0.18	1.29	1.66	2.35
26	686	<2	Ss/SPs	10.45	30.89	5.83	1.46	1.14	0.10	2.71	5.30	14.99
27	686	2-4	Ss/SPs	10.41	27.00	9.36	1.02	0.98	0.13	2.13	2.89	5.38
28	686	4-6	SEr	10.67	26.55	7.16	1.19	1.00	0.09	2.29	3.71	8.73
29	686	6-8	DBr	13.13	19.85	7.96	0.75	0.65	0.08	1.49	2.49	5.46
30	691A	<2	Sr	10.42	30.60	6.73	1.41	1.35	0.10	2.86	4.55	11.26
31	691A	2-4	SPr	10.87	28.96	6.52	1.27	1.18	0.09	2.54	4.44	11.36
32	691A	4-6	DBr	9.45	27.85	6.98	1.25	1.14	0.09	2.48	3.99	9.58
33	691A	6-8	SEr	18.22	19.02	8.36	0.64	0.63	0.09	1.36	2.27	4.80
34	691A	>10	Tr	14.81	21.52	12.00	0.61	0.66	0.15	1.41	1.79	2.84
35	691B	<2	Sr	12.35	31.81	7.22	1.39	1.26	0.12	2.76	4.41	10.22
36	691B	2-4	Sr	13.93	31.30	8.29	1.16	1.11	0.13	2.39	3.78	7.74
37	691B	4-6	SEr	14.03	31.74	6.50	1.43	1.25	0.10	2.79	4.88	12.47
38	691C	<2	Sr	8.88	29.12	5.81	1.44	1.41	0.10	2.95	5.01	14.25
39	691C	2-4	SPr	9.96	28.01	7.76	1.21	1.13	0.12	2.47	3.61	7.89
40	691D	<2	Sr	12.12	25.49	5.42	1.27	1.27	0.11	2.65	4.70	14.34
41	691D	2-4	SPr	10.20	22.92	5.30	1.13	1.15	0.11	2.39	4.32	13.49
42	691D	4-6	SEr/ISs	12.61	18.42	5.45	1.02	1.03	0.08	2.13	3.38	10.38
43	691D	6-8	DBr	15.04	23.98	12.55	0.63	0.67	0.14	1.45	1.91	2.88
44	691D	8-10	DBr	13.85	18.53	16.58	0.31	0.35	0.15	0.82	1.12	1.53
45	692A	<2	SPr	9.18	22.97	4.20	1.49	1.22	0.10	2.81	5.48	21.33
46	692A	4-6	DBr	10.58	28.69	10.61	0.98	0.96	0.15	2.09	2.71	4.53

(Table continues on next page)

47	692B	<2	Sr	10.44	31.23	5.01	1.64	1.30	0.09	3.03	6.24	20.37
48	692B	2-4	DBr	10.74	26.33	6.10	1.21	1.16	0.09	2.45	4.32	11.78
49	692B	>10	Ir	9.21	25.57	11.26	0.48	0.78	0.16	1.43	2.27	3.68
50	692C	<2	Sr	7.04	20.33	6.15	1.13	1.18	0.15	2.46	3.30	9.06
51	692C	2-4	Sr	9.80	19.87	8.45	1.03	0.95	0.16	2.14	2.35	4.90
52	692C	4-6	Ir/Tr	13.12	26.08	12.70	0.64	0.70	0.18	1.53	2.05	3.04
53	692D	<2	Sr	11.55	28.46	7.28	1.28	1.30	0.11	2.68	3.91	9.03
54	692D	2-4	SPr	10.74	29.80	6.84	1.36	1.28	0.10	2.75	4.36	10.65
55	692D	4-6	TBr	10.93	26.42	7.12	1.18	1.06	0.10	2.34	3.71	8.80
56	693	<2	Sr	11.51	30.59	8.81	1.24	1.24	0.16	2.64	3.47	6.76
57	693	2-4	Sr	9.56	30.48	8.13	1.21	1.27	0.13	2.62	3.75	7.83
58	693	4-6	Vr	14.56	22.34	15.06	0.47	0.48	0.18	1.13	1.48	2.02
59	695	<2	Sr	20.07	31.59	8.56	1.29	1.25	0.12	2.66	3.69	7.35
60	695	2-4	SPr	16.60	32.75	6.35	1.45	1.21	0.09	2.75	5.16	13.45
61	695	4-6	DBr	12.96	28.90	7.86	1.27	1.22	0.09	2.80	3.68	7.94
62	696	<2	Sr	9.80	30.98	5.54	1.52	1.29	0.10	2.91	5.59	16.58
63	696	2-4	SEr	10.33	29.84	6.40	1.42	1.28	0.11	2.81	4.66	12.12
64	696	4-6	Tr	11.36	27.92	6.22	1.26	1.26	0.12	2.63	4.48	11.99
65	699	<2	Sr	10.17	29.26	6.55	1.56	1.16	0.10	2.81	4.47	12.46
66	699	2-4	Sr	10.03	29.74	6.29	1.53	1.18	0.09	2.80	4.73	11.37
67	699	4-6	SEr	10.87	28.86	6.52	1.39	1.18	0.09	2.66	4.43	11.32
68	700	<2	Sr	6.72	31.30	6.78	1.54	1.39	0.10	3.04	4.62	11.34
69	700	4-6	SPr	11.93	27.57	8.43	1.11	0.95	0.09	2.16	3.27	6.65
70	700	6-8	SEr	11.18	29.87	7.70	1.29	1.11	0.10	2.50	3.88	8.51
71	704A	<2	Sr	9.37	30.37	5.42	1.37	1.16	0.10	2.63	5.60	16.98
72	704A	2-4	SPr	9.97	26.41	5.88	1.34	1.16	0.09	2.59	4.49	12.67
73	704A	4-6	SPr	11.05	29.41	5.95	1.15	1.12	0.08	2.35	4.95	13.73
74	704A	6-8	TBr	13.25	23.11	12.28	0.28	0.60	0.18	1.06	1.88	2.90
75	704A	8-10	DBr	14.17	22.71	11.65	0.57	0.63	0.17	1.36	1.95	3.13

(Table continues on next page)

Table 1 (continued)

Sr. No.	Station No.	Size (cm)	Nodule type ^a	Moisture (%)	Mn (%)	Fe (%)	Cu (%)	Ni (%)	Co (%)	(Cu + Ni + Co) (%)	Mn/Fe	Growth rate (mm/ma)
76	704A	>10	TDB	16.76	22.28	12.81	0.42	0.50	0.18	1.10	1.74	2.62
77	704B	<2	Sr	12.99	32.83	7.10	1.34	1.23	0.11	3.69	4.63	10.88
78	704B	2-4	SPr	14.50	30.23	6.36	1.38	1.19	0.09	2.66	4.75	12.39
79	704B	4-6	Ebr	13.60	28.43	6.13	1.32	1.17	0.08	2.58	4.51	12.56
80	704B	6-8	Ebr	14.62	16.42	6.29	0.44	0.54	0.07	1.05	2.61	7.09
81	704B	>10	DB	17.41	20.46	11.31	0.51	0.57	0.15	1.22	1.81	3.01
82	704C	<2	Sr	12.40	27.97	8.98	1.12	1.02	0.13	2.27	3.11	6.00
83	704C	2-4	SPr	12.60	28.64	7.74	1.28	1.20	0.13	2.61	3.70	8.10
84	704C	4-6	DBr	12.35	25.49	9.31	0.97	0.89	0.14	2.00	2.74	5.15

^aMorphological symbols: S, spheroidal; E, ellipsoidal; D, discoidal; P, poly or intergrown; I, irregular; V, variable; F, faceted; B, biological; T, tabular or flattened. Surface texture symbols: s, smooth; r, rough.

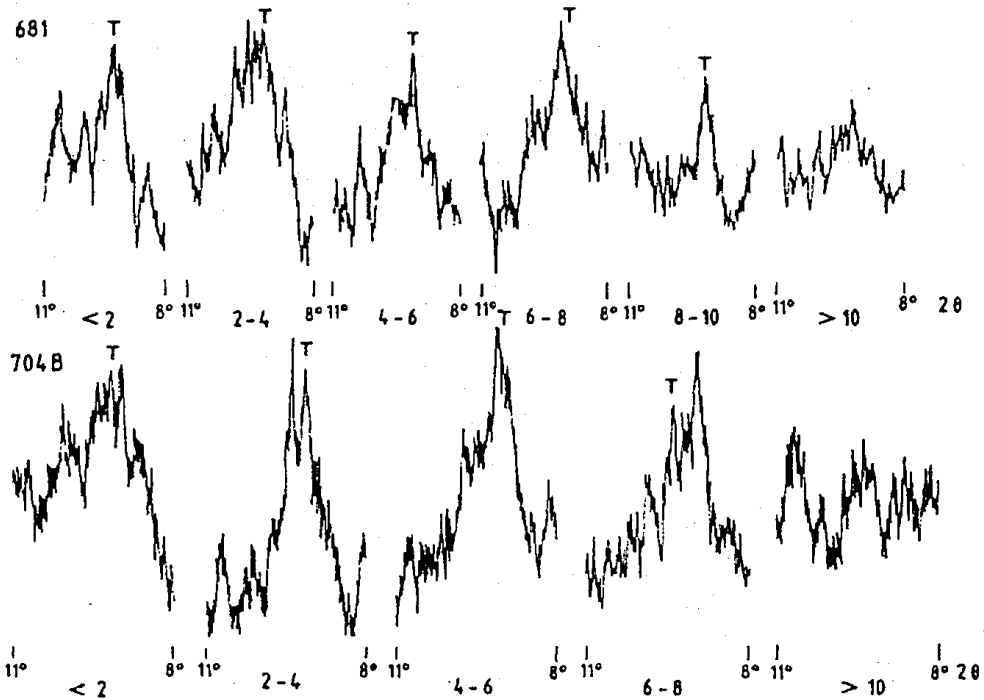


Figure 3. X-ray diffractograms of the polymetallic nodules.

there are 22 sets consisting of 22 samples from class 1, 21 from class 2, 19 from class 3, 11 from class 4, 4 from class 5, and 7 from class 6.

Tables 1 and 3 and Figures 4 and 5 show a clear correlation between bulk nodule composition and size. Closer examination revealed the following:

1. Higher metal content (grade) is observed for the size classes 1 and 2.
2. The metal content decreases with increasing size class.
3. 86% of class 1 and 64% of class 2 nodules have more than 2.47% of the total (Cu + Ni + Co) content.
4. Iron and moisture content increase with nodule size.

There is gradual increase in Fe content with increase in nodule size, whereas Mn shows gradual decrease. It appears that the inverse relationship of Mn with Fe has secondary control of the nodule size. The Mn/Fe ratio decreases with an increase in nodule size and is well documented in Table 3.

The results described here are quite different from those of the Pacific Ocean nodules. Friedrich et al. (1983) studied mature (bigger) and immature (smaller) nodules from the Clarion-Clipperton fracture zone and found that the smaller nodules are characterized by high Mn/Fe ratios (average 4.8) and high Cu + Ni contents (average 2.54%) but low abundance (average 1.3 kg/m^{-2}) of lower Miocene age, whereas Mn, Fe, Co, and Zn showed no systematic trend. The present study shows a systematic decrease in Mn, Cu, Ni, and Co, whereas Fe and the moisture content increase with the nodule size. The smaller nodules have a high (Cu + Ni + Co) percentage and are more abundant than the bigger ones. Similar studies on the nodules of 3- to 6-cm from the southwestern Carlsberg Ridge showed that with increasing diameter the Mn, Cu, and Co content increase, whereas Fe and Zn decrease and Ni has no significant trend (Valsangkar et al.

Table 2
Elemental Ranges (%) of Nodules from the Central Indian Ocean Basin

Element	Nodule class						All classes
	1 (<2 cm)	2 (2-4 cm)	3 (4-6 cm)	4 (6-8 cm)	5 (8-10 cm)	6 (>10 cm)	
Moisture	6.72-20.07	9.56-16.60	9.45-16.21	8.46-18.59	13.52-19.66	9.21-20.21	6.72-20.21
Mn	20.33-32.83	19.87-32.75	18.42-31.74	16.42-29.87	17.02-25.29	20.46-25.57	16.42-32.83
Fe	4.20-8.98	6.10-13.16	5.45-15.06	6.29-13.96	7.87-16.58	7.38-12.81	4.19-16.58
Cu	1.23-1.56	0.65-1.53	0.47-1.44	0.28-1.29	0.31-0.89	0.42-0.89	0.28-1.64
Ni	1.02-1.39	0.65-1.35	0.48-1.29	0.54-1.11	0.35-0.86	0.50-0.84	0.35-1.41
Co	0.09-0.16	0.09-0.12	0.08-0.18	0.07-0.18	0.08-0.17	0.11-0.18	0.07-0.18
Cu + Ni + Co	2.66-3.69	1.47-3.03	1.13-2.82	1.05-2.50	0.82-1.89	1.10-1.83	0.82-3.69
Mn/Fe	3.11-6.24	1.86-5.02	1.48-4.88	1.66-3.88	1.12-2.43	1.74-3.08	1.12-6.24
Cu + Ni	2.14-2.94	1.30-2.94	0.95-2.73	0.88-2.40	0.67-1.75	0.92-1.72	0.67-2.94

Table 3
Average Elemental Concentrations (%) of Nodules from the Indian and Pacific Ocean Nodules

Element	Nodule class						All classes	Equatorial NE Pacific Ocean nodules ^a
	1 (<2 cm)	2 (2-4 cm)	3 (4-6 cm)	4 (6-8 cm)	5 (8-10 cm)	6 (>10 cm)		
Moisture	11.33	11.77	12.49	14.39	15.30	15.64	12.65	NA ^b
Mn	29.08	28.26	27.19	23.86	20.89	22.55	26.83	22.40
Fe	6.69	7.44	8.09	9.08	11.63	10.45	8.06	8.10
Cu	1.39	1.24	1.14	0.83	0.59	0.62	1.12	1.02
Ni	1.23	1.13	1.04	0.80	0.60	0.69	1.03	1.16
Co	0.11	0.12	0.11	0.12	0.14	0.14	0.12	0.25
Cu + Ni + Co	2.77	2.49	2.29	1.74	1.32	1.47	2.28	2.43
Mn/Fe	4.48	3.98	3.60	2.77	1.92	2.23	3.63	2.76
Cu + Ni	2.62	2.37	2.18	1.63	1.19	1.30	2.15	NA

^aGlasby et al. (1986).

^bNA, data not available.

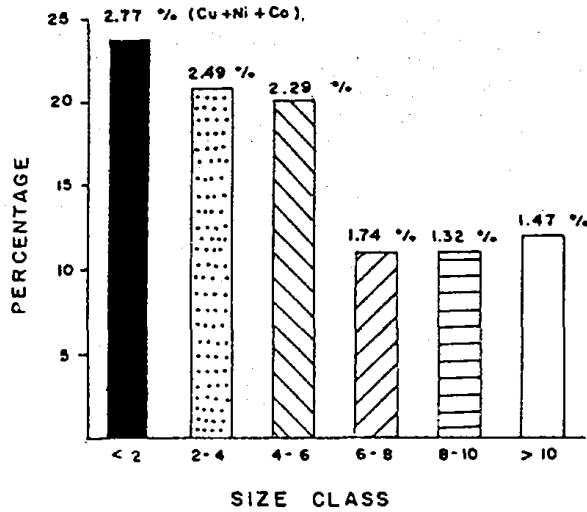


Figure 4. Histograms showing modal distribution of grade and nodule size.

1988). The environmental conditions and formation mechanism of the Carlsberg Ridge nodules are different from that of the CIOB nodules.

Interelement Relationships

The interelement relationships for each nodule class along with whole data is given in Tables 4A-G. Several strong correlations can be seen, and the general trends are similar

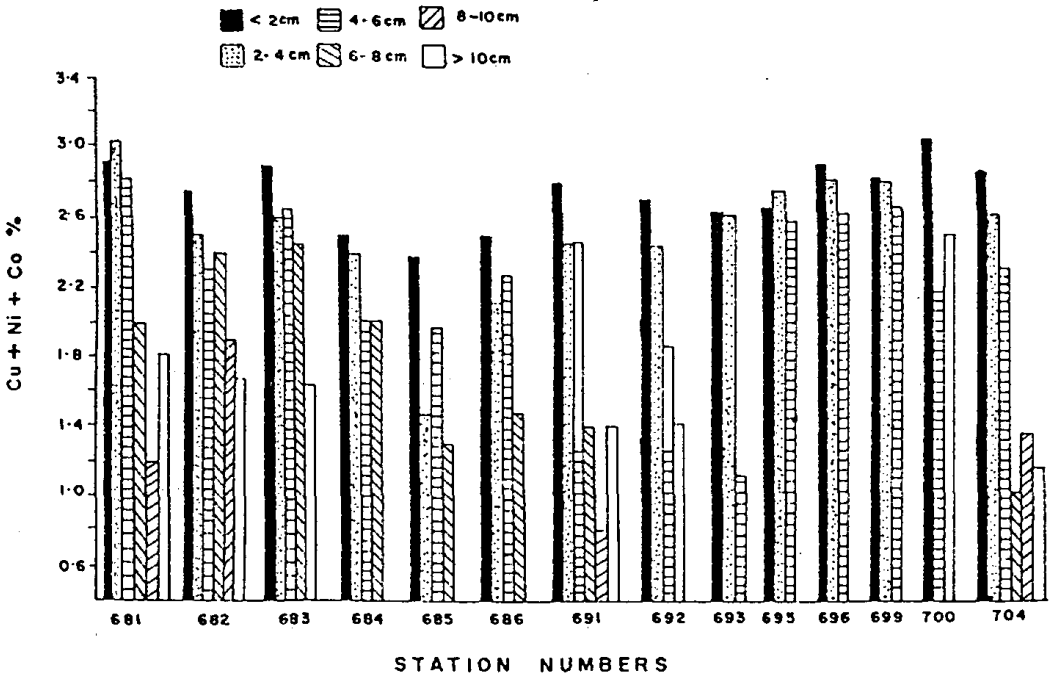


Figure 5. Histograms showing correlation between size class and grade for SS-13 nodules.

Table 4A
 Interelement Relationship in the CIOB Nodules:
 Class 1 (<2 cm)^a

	Mn	Fe	Cu	Ni	Co	Cu + Ni + Co	Mn/Fe
H ₂ O	.44	.52	-.16	-.22	.09	-.59	-.24
Mn		.33	.31	.14	-.28	.37	.28
Fe			-.59	-.39	.60	-.35	-.80
Cu				.49	-.76	.59	.77
Ni					-.42	.57	.40
Co						-.46	-.76
Cu + Ni + Co							.52

^aN = 22, r = 0.40, CL = 95%.

Table 4B
 Interelement Relationship in CIOB Nodules:
 Class 2 (2-4 cm)^a

	Mn	Fe	Cu	Ni	Co	Cu + Ni + Co	Mn/Fe
H ₂ O	.46	.05	.14	-.01	-.05	-.08	.24
Mn		-.24	.59	.56	-.44	.60	.59
Fe			-.84	-.82	.89	-.84	-.89
Cu				.89	-.83	.98	.91
Ni					-.75	.97	.85
Co						-.79	-.92
Cu + Ni + Co							.90

^aN = 21, r = 0.41, CL = 95%.

Table 4C
 Interelement Relationship in CIOB Nodules:
 Class 3 (4-6 cm)^a

	Mn	Fe	Cu	Ni	Co	Cu + Ni + Co	Mn/Fe
H ₂ O	-.05	.35	-.22	-.22	.27	-.22	-.26
Mn		-.32	.65	.59	-.22	.65	.61
Fe			-.87	-.90	.91	-.88	-.90
Cu				.96	-.78	.99	.90
Ni					-.78	.99	.92
Co						-.76	-.81
Cu + Ni + Co							.91

^aN = 19, r = 0.43, CL = 95%.

Table 4D
Interelement Relationship in CIOB Nodules:
Class 4 (6–8 cm)^a

	Mn	Fe	Cu	Ni	Co	Cu + Ni + Co	Mn/Fe
H ₂ O	-.34	.04	-.27	-.27	-.13	-.29	-.29
Mn		—	.78	.86	.26	.85	.65
Fe			-.54	-.48	.90	-.47	-.76
Cu				.96	-.35	.99	.92
Ni					-.22	.99	.92
Co						-.24	-.50
Cu + Ni + Co							.91

^aN = 11, r = 0.55, CL = 95%.

Table 4E
Interelement Relationship in CIOB Nodules:
Class 5 (8–10 cm)^a

	Mn	Fe	Cu	Ni	Co	Cu + Ni + Co	Mn/Fe
H ₂ O	-.70	-.67	-.08	-.18	-.93	-.21	.26
Mn		-.06	.74	.82	.57	.83	.51
Fe			-.65	-.60	.70	-.57	-.88
Cu				.99	-.13	.99	.92
Ni					—	.99	.90
Co						.01	-.38
Cu + Ni + Co							.89

^aN = 4, r = 0.81, CL = 95%.

Table 4F
Interelement Relationship in CIOB Nodules:
Class 6 (>10 cm)^a

	Mn	Fe	Cu	Ni	Co	Cu + Ni + Co	Mn/Fe
H ₂ O	-.81	-.35	.10	-.22	-.54	.07	.11
Mn		-.08	.09	.54	.22	.29	.36
Fe			-.78	-.80	.93	-.91	-.95
Cu				.68	-.71	.88	.78
Ni					-.68	.92	.87
Co						-.83	-.79
Cu + Ni + Co							.92

^aN = 7, r = 0.67, CL = 95%.

Table 4G
Interelement Relationship in CIOB Nodules:
Whole Data^a

	Mn	Fe	Cu	Ni	Co	Cu + Ni + Co	Mn/Fe
H ₂ O	-.26	.35	-.44	-.48	.07	-.45	-.41
Mn		-.39	.77	.76	-.23	.79	.71
Fe			-.80	-.79	.81	-.78	-.81
Cu				.95	-.58	.97	.92
Ni					-.51	.97	.89
Co						-.51	-.66
Cu + Ni + Co							.90

^a*N* = 84, *r* = 0.21, CL = 95%.

to those reported. Positive correlations between Mn, Cu, Ni, and Mn/Fe and between Fe and Co are encountered for six nodule classes and also for the whole data. The whole data (Table 4G) show that Mn correlates strongly with Cu, Ni, (Cu + Ni + Co), and Mn/Fe ratios. Excellent correlation is seen between Cu and Ni (+0.95) and Fe and Co (+0.81). Another excellent correlation exists between Mn/Fe and Cu (+0.91) and Ni (+0.88), whereas Mn and Fe show an inverse relationship. It may be noted that in class 1 nodules (Table 4A), the positive correlation of Mn with Fe, Cu, Ni, and Mn/Fe is not significant. In class 5 nodules (Table 4E), Mn correlates with Ni significantly, whereas in class 6 nodules (Table 4F), Mn does not have significant correlation.

Significant positive correlation is observed between Fe (Table 4G) and Co. The moisture content also shows positive correlation with some of the elements. The correlation of moisture with Fe is obscure in Tables 4A and 4G.

Similar results can be obtained from Figures 6–8 where whole data plots for Cu and Ni, Fe and Co, Mn and Ni, and Mn and Cu show strong positive relationships (Figure 6a–d), whereas Ni and Co, Mn and Fe, and Fe and Ni are negatively correlated (Figures 6e, f and 7a). Mn and Ni correlates positively with Mn/Fe (Figures 8a and 7e), whereas Fe and Co correlation is negative (Figure 8b, c). It is interesting to note that while Mn/Fe correlation with Co is negative (Figure 8c), that with combined (Cu + Ni + Co) is positive (Figure 7f). Similarly, correlation of (Cu + Ni + Co) with Mn is positive (Figure 7b), whereas that with Fe is negative (Figure 7c). This indicates strong association of Fe with Co alone.

Discussion

It is clear from the preceding sections that the nodule composition is principally related to the nodule size. The morphology of nodules is also controlled by the size parameter. With the increase in size the shape changes from spheroidal (class 1) to ellipsoidal (class 2). The degree of sphericity also varies with the nodule class and is inversely proportional to the size. With increase in the diameter, the nodules become progressively flattened, elongated, tabular, and irregular. This observation is similar to that of Raab (1972). The data thus indicate that the morphology is related to the nodule dimension. The spheroidal and ellipsoidal nodules with rough surface textures belonging to classes 1 and 2 have highest chemical concentration of the analyzed elements. Glasby et al. (1982) also ob-

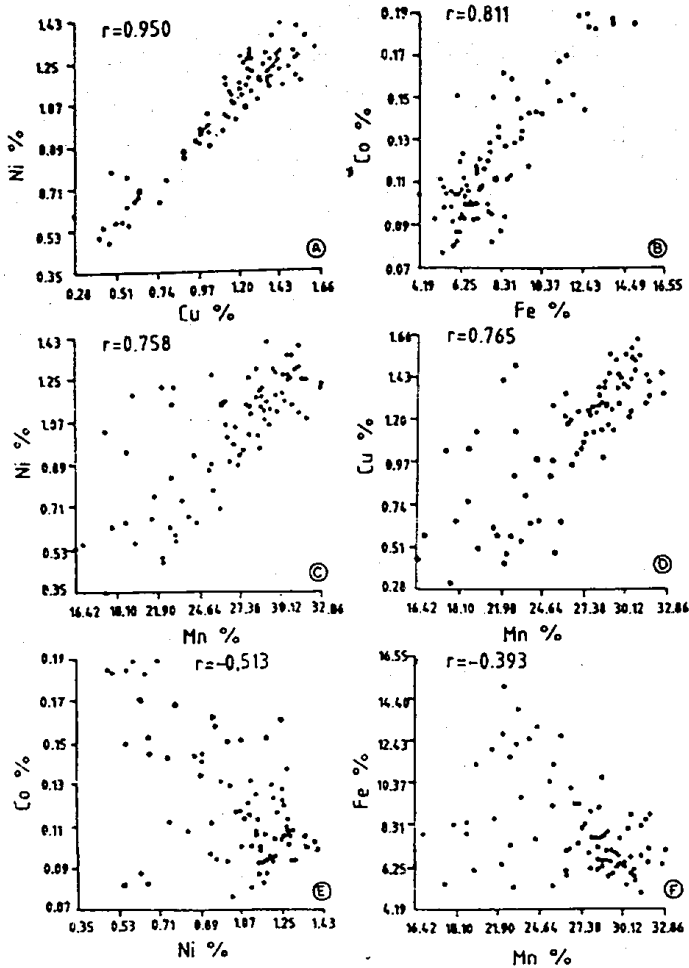


Figure 6. Variation of (a) Cu with Ni, (b) Fe with Co, (c) Mn with Ni, (d) Mn with Cu, (e) Ni with Co, (f) Mn with Fe.

served similar compositional variations for three different nodule types and found that the variability of nodule composition is related to the nodule morphology.

In manganese nodules, the incorporation of transition metals is controlled by the mineralogy (Usui 1979). The divalent metal ions (Cu and Ni) are usually associated with the 10° manganite (todorokite) phase. Therefore, the presence of todorokite mineral becomes important when considering nodule composition. The abundance of todorokite decreases with higher class nodules; this is revealed from the relative intensity of the XRD peaks (Figure 3). The decreasing composition of nodules with increasing size is therefore controlled by the todorokite abundance. The supply of divalent trace metal ions during diagenesis controls the formation of todorokite and the nodule composition (Glasby and Thijssen 1982). If this is true, then in the present case the decreasing composition and abundance of todorokite with increasing nodule class indicate that the higher classes are less affected by the diagenetic processes.

The difference in the size, shape, and surface characteristics of the nodule types could be because of their rolling nature on the seafloor (Halbach and Öskara, 1979). As mentioned above, the rolling characteristic is also related to the nodule size. Class 1 nodules are normally spheroidal and with increasing size class the shape and surface texture

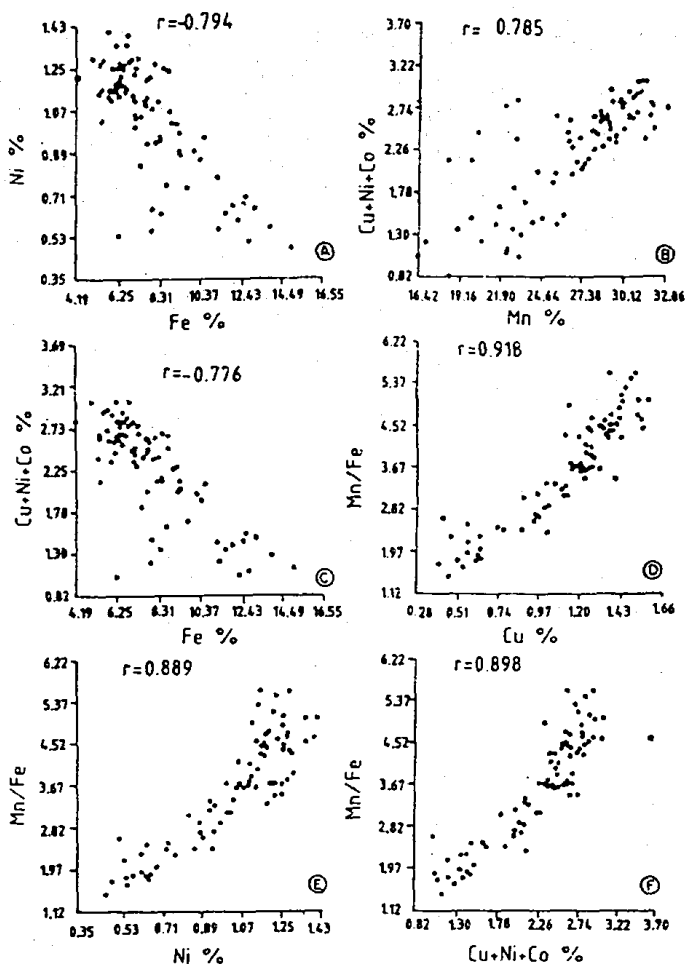


Figure 7. Variation of (a) Fe with Ni, (b) Mn with Cu + Ni + Co, (c) Fe with Cu + Ni + Co, (d) Cu with Mn/Fe, (e) Ni with Mn/Fe, (f) Cu + Ni + Co with Mn/Fe.

changes. Bigger nodules are more stable than the smaller nodules; therefore, they receive metals both from the sea and pore waters. The rolling nature may be favorable for the nodules of classes 1 and 2 only.

The large variation of Mn/Fe ratios from 1.1 to 6.2 indicates multiple source of supply of the elements by different accretionary process and early diagenesis (Halbach et al. 1981). According to Sorem et al. (1979), the diagenetic supply of transition elements would be more pronounced in larger nodules embedded at the sediment-water interface leading to enrichment of these elements and todorokite. By this hypothesis, the smaller nodules should not have been enriched in Cu and Ni and also in todorokite. The present data thus suggest that the diagenetic process is not related to nodule size. As compared to larger nodules (classes 3-6) the smaller ones (classes 1 and 2) have a higher content of Cu + Ni + Co (2.77 and 2.49% respectively, Table 3, Figure 4) and higher Mn/Fe ratios (4.48 and 3.98, respectively), which suggests that these nodules were in contact with the sediment-water interface for a longer time. The decreasing abundance and crystallinity of todorokite with increasing nodule size also supports this view. The rolling characteristic of class 1 and 2 nodules therefore favors the nodules to remain in contact with the sediments leading to diagenesis and thereby enrichment of metal ions. In the

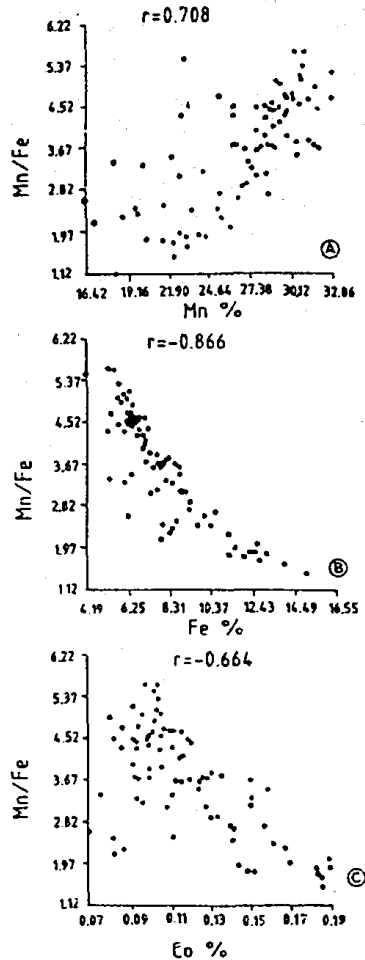


Figure 8. Variation of (a) Mn with Mn/Fe, (b) Fe with Mn/Fe, (c) Co with Mn/Fe.

higher size classes, because of their static nature and partial contact with sediment surface, such diagenetic supply would be limited, which further leads to lowering of Mn/Fe ratios, Cu and Ni contents, and the lower todorokite abundances.

Nodule composition may also be related to the sediment thickness. According to Calvert et al. (1978), the nodules associated with thin Quarternary sediments are more diagenetic in nature. In the present case, this hypothesis indicates that the smaller nodules are associated with the thin sediment layer and the bigger ones with the thick sediment layer. Because all the nodule size classes are obtained by dredging an area of less than 1 km distance on the seafloor during every operation, the sediment thickness variation and the topographical variation to such an extent is not expected. Although it is possible that the nodules of different sizes are mixed together because of the dredging, our earlier exploration survey for number of spot sampling in CIOB shows that the area consists of association of smaller and bigger nodules.

The possibility of class 1 and 2 nodules brought in contact with more static nodules of classes 3–6 from outside because of strong bottom currents cannot be ruled out. The smaller nodules of classes 1 and 2 in such a situation could have grown faster in the area of very high productivity. The calculated growth rates (Table 1) support this view. The

present data indicate that the growth rates are inversely proportional to the nodule size. Heye and Marchig (1977) observed positive correlation between growth rates and Mn/Fe ratios and further noticed that the fast-growing layers were enriched in Mn, Cu, and Ni. In the present case, this relationship exists only for class 1 and 2 nodules.

The sampling area consists of siliceous ooze sediments (Udintsev 1975), which represent a zone of high biological productivity. The high Mn/Fe ratios up to 6.24 (average 3.63) and high Cu + Ni contents up to 2.94 (average 2.14) also support the high productivity in the area. Siliceous diatomaceous organisms when decomposed on the seafloor release Mn, Cu, and Ni. These elements are available in the area where nodules are growing and act as an additional supply of elements that will be incorporated through pore waters during diagenesis. The porous structure of nodules and sediments tends to help the movement of pore water. The accretion of nodules under such conditions should be faster. The biological productivity in the area may be localized so that the class 3–6 nodules growing in a similar environment receive a major supply of the elements through seawater. Jauhari (1987) has also suggested high biogenic flux to be responsible for the high concentration of Cu, Ni, and Mn in the nodules. The equatorial north Pacific nodules from the Clarion-Clipperton fracture zone, which appears to have the most promising commercial deposits, also show variations in the morphology, internal structure, mineralogy, and composition; and the variations in the biological productivity in the overlying waters are considered as the main reason (Friedrich et al. 1983). Possibility of similar situations in the southern latitudes in the Indian Ocean cannot be ruled out.

Frazer and Fisk (1981) and Glasby et al. (1982) found the nodule composition to be a function of water depth. The water depth in the area ranges from 5025 to 5500 m and the nodule morphology was found to be constant with water depth. Probably, the observations of these authors could be very much localized as compared with the large-area coverage in the present study. Such observations could be misleading and therefore should be carefully established for a sufficiently large area.

Nodules with high Mn/Fe ratios are associated with low sedimentation rates (Piper and Williamson 1977) and are reported to be a function of water depth (Glasby et al. 1982). The large variation in the Mn/Fe ratios (1.12–6.24, Table 2) obtained in the present study therefore indicates variable rates of sedimentation in the area. A higher Mn/Fe ratio also stabilizes the formation of todorokite (Glasby et al. 1982) and is in accordance with the present finding. The sedimentation rates determined for four cores from the CIOB varied from 1 to 9 mm/10³ years (Borole, personal communication). This variation is thought to be because of the effect of bottom currents and variation in the sedimentary processes.

The results obtained and discussed in this article should be considered when assessing an area for a potential mine site. Manganese nodule grades and abundance are normally negatively correlated both regionally and locally in the Pacific Ocean (Menard and Frazer 1978, Mizuno 1981) and in the Indian Ocean (Sudhakar 1988, Pattan and Kodagali 1988). Such correlation for a 71 424-km² area in the present case showed interesting results that are presented in Figure 2. The selected size classes show that class 1 and 2 nodules are most abundant in the area and are above paramarginal grade (Cu + Ni + Co percentage). The inverse relationship observed by other authors therefore must not be applied to the selective nodule size classes as discussed in the present study. It therefore becomes necessary to reestablish such correlation because the future of ocean mining depends on, among other factors, the magnitude of the distribution patterns of nodules both in grade and abundance.

Conclusions

1. Morphology of the nodules depends upon the size of the nodules. The morphological classification, therefore, should be based primarily on the size parameters of the nodules rather than by their description (Meyer 1973, Moritani et al. 1977, Halbach and Öskara 1979).

2. The CIOB has different types of nodule population, ranging from less than 2 cm (class 1) to more than 10 cm (class 6) but class 1 and 2 size nodules are most abundant.

3. Spheroidal and ellipsoidal nodules with rough surfaces (Sr) are more abundant than smooth ones (Ss).

4. The principal manganese oxide phase is todorokite, which is more abundant than burnessite and δ - MnO_2 . Todorokite abundance decreases with increasing size class, whereas δ - MnO_2 behaves independently.

5. The chemical composition shows an inverse relationship with nodule size. Mn, Cu, Ni, and Co concentrations increase from class 6 to class 1 nodules. Spheroidal and ellipsoidal nodules with rough surface texture (Sr/Ser) have the highest elemental composition. Iron and moisture content increases with the nodule size.

6. Mn correlates strongly with Cu, Ni, and Mn/Fe ratio; and Fe with Co. Mn and Fe are negatively correlated.

7. The class 1 and 2 nodules are formed with an additional source of supply, probably under high biological activity, and rolled and mixed with other nodule classes (3-6) associated with siliceous sediments.

8. High Mn/Fe ratios obtained for smaller nodules suggest a diagenetic process of formation. Although in the triangular diagram (Figure 9) all the plots occupy the hydro-

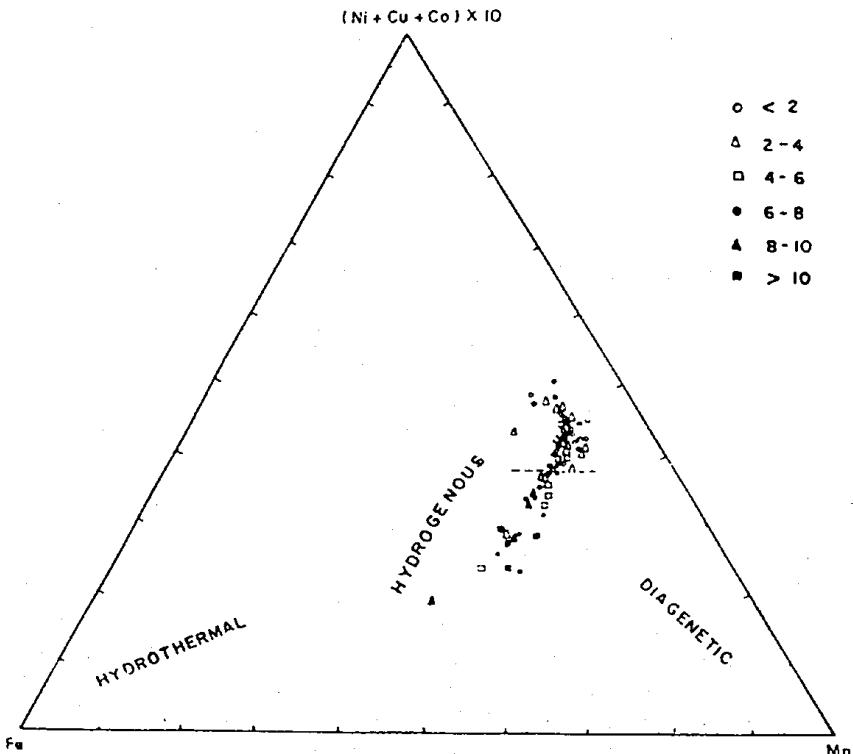


Figure 9. Fe-Mn-(Cu + Ni + Co) \times 10 triangular diagram. The dashed line separates the field occupied by the bigger nodules (classes 4-6) from the smaller ones (classes 1-3).

genous field, a clear distinction can be made between <2- to 6-cm and 6- to >10-cm nodules. A multiple source of supply is therefore responsible for the formation of these nodules.

9. Higher Mn/Fe ratios, higher values of Mn, Cu, and Ni, and enrichment of todorokite further imply replacement of structures by oxides and cavity fillings. This needs confirmation by SEM studies.

10. Higher growth rates and enrichment in Mn, Cu, and Ni for class 1 and 2 nodules as compared to the other classes (3–6) indicate an additional supply of elements during formation. The nodules of classes 3–6 indicate formation at comparatively slower rates and probably at the expense of the smaller nodules.

11. Class 1 and 2 nodules have high economic potential (above 2.49% grade) and show maximum abundance (86.3 and 64.6%, respectively). This further suggests that the nodules of classes 1 and 2 are most feasible for the commercial exploitation. The size parameter will have to be considered when designing the nodule collector because it has direct impact on metallurgical studies.

12. Similarity in the composition, morphology, and mineralogy of the nodules with those from the northeast Pacific economic zone indicates that similar environmental conditions should have existed in the southern latitudes in the Indian Ocean.

Acknowledgments

The authors are thankful to Shri R. R. Nair for his keen interest, encouragement, and suggestions. Thanks also to Shri N. H. Hashimi for help in XRD and A. L. Paropkari and V. K. Banakar in A. A. S. analyses. Help rendered by the participants of SS-13 cruise during sample collection, Shri P. G. Mislankar in sample preparation, Shri V. M. Date in printing, and Shri S. Akerkar in preparation of figures is gratefully acknowledged. The research was carried out with financial support by the D.O.D., New Delhi, under the program of Surveys for polymetallic nodules.

References

- Andrews, J. E., and G. H. W. Friedrich. 1979. On the sedimentation in the northern part of the south Pacific. In *Oceanography of the South Pacific*, R. Frazer, comp. Washington, DC: National Commission for UNESCO, pp. 217–219.
- Barnes, S. S. 1967. Minor-element composition of ferromanganese nodules. *Science* 157:63–65.
- Burns, V. M., R. G. Burns, and W. K. Zwicker. 1975. Classification of natural manganese dioxide minerals. In *Proceedings, International Symposium on manganese dioxide minerals*, A. Kozawa and R. G. Brodd, eds., Cleveland, OH: Electrochemical Society Publishing Co.: Electrochemical Society, pp. 288–305.
- Calvert, S. E., N. B. Price, G. R. Heath, and T. C. Moore. 1978. Relationship between ferromanganese nodule composition in a small survey area of equatorial Pacific. *J. Marine Res.* 36:161–183.
- Cronan, D. S., and S. A. Moorby. 1981. Manganese nodules and other ferromanganese oxide deposits from the Indian Ocean. *J. Geol. Soc. London* 138:527–539.
- Cronan, D. S., and J. S. Tooms. 1969. The geochemistry of manganese nodules and associated pelagic deposits from the Pacific and Indian Oceans. *Deep-Sea Res.* 16:335–359.
- Frazer, J. Z., and M. B. Fisk. 1981. Geological factors related to characteristics of sea-floor manganese nodule deposits. *Deep-Sea Res.* 28A:1533–1551.
- Frazer, J. Z., and L. L. Wilson. 1980. Manganese nodule resources in the Indian Ocean. *Mar. Min.* 2:257–291.

- Friedrich, G., G. P. Glasby, T. Thijssen, and W. L. Plüger. 1983. Morphological and geochemical characteristics of manganese nodules collected from the three areas on an equatorial Pacific transect by R. V. Sonne. *Mar. Min.* 4:167-254.
- Glasby, G. P., and T. Thijssen. 1982. Control of the mineralogy and composition of marine manganese nodules by the supply of divalent transition metal ions. *Neues jahrbuch fur mineralogie*, 145:291-307.
- Glasby, G. P., G. Friedrich, T. Thijssen, W. L. Plüger, H. Kunzendorf, A. K. Gosh, and G. S. Roonwal. 1982. Distribution, morphology and geochemistry of manganese nodules from the Valdivia 13/2 area, equatorial north Pacific. *Pacific Science* 36:241-263.
- Glasby, G. P., N. F. Exon, and M. A. Meylan. 1986. Manganese nodules in the S W Pacific. In *Sedimentation and mineral deposits in the southwestern Pacific Ocean*, D. S. Cronan, ed. Florida: Academic, pp. 237-262.
- Halbach, P., and M. Öskara. 1979. Morphological and geochemical classification of deep-sea ferromanganese nodules and its genetical interpretation. In *La genese des Nodules de Manganese, 1978*. Centre National de la Recherche Scientifique, Paris: CNRS vol. 289, pp. 77-88.
- Halbach, P., C. Scherhag, U. Hebisch, and V. Marchig. 1981. Geochemical and mineralogical control of different genetic types of deep-sea nodules from the Pacific Ocean. *Mineralium Deposita* 16:59-84.
- Heye, D. 1979. Relationship between the size of manganese nodules in the Central Pacific, their chemical constitution and other parameters. In *La genese des nodules de manganese, 1978*. Colloques internationaux du Centre de la Recherche Scientifique, Paris: CNRS vol. 289, pp. 89-91.
- Heye, D., and V. Marchig. 1977. Relationship between the growth rate of manganese nodules from the Central Pacific and their chemical constitution. *Mar. Geol.* 23:M19-25.
- Jauhari, P. 1987. Classification and inter-element relationships of ferromanganese nodules from the Central Indian Ocean basin. *Mar. Min.* 6:419-429.
- Lyle, M. 1982. Estimating growth rates of ferromanganese nodules from chemical composition: Implications for nodule formation processes. *Geochim. Cosmochimi. Acta* 46:2301-2306.
- Menard, H. W., and J. Z. Frazer. 1978. Manganese nodules on the sea floor: Inverse correlation between grade and abundance. *Science* 199:969-971.
- Mero, J. L. 1965. *The mineral resources of the sea*. Amsterdam: Elsevier, 312 pp.
- Meyer, K. 1973. Surface sediment and manganese nodule facies, encountered on 'R. V. Valdivia' Cruises 1972/73. *Mar. Technol.* 4:196-199.
- Mizuno, A. 1981. Regional and local variabilities of manganese nodules in the Central Pacific Basin, January-March, 1979 (GH 79-1 Cruise). In *Geol. Surv. Japan*, A. Mizuno, ed. Cruise report 15; pp. 281-296.
- Mizuno, A., and T. Moritani. 1978. Manganese nodule deposits of the Central Pacific. In *Fifth international ocean development conference, Tokyo, Japan*, vol. 2, pp. 27-39.
- Moritani, T., S. Maruyama, M. Nohara, K. Matsumoyo, T. Ogitsu, and H. Moritani. 1977. Description, classification and distribution of manganese nodules. In *Deep sea mineral sources investigation in the Central-Eastern part of Central Pacific Basin, January-March 1976, (GH 76-1 Cruise)*. *Geol. Surv. Japan*, A. Mizuno and T. Moritani, eds. Cruise Report 18, pp. 136-158.
- Pattan, J. N., and V. N. Kodagali. 1988. Seabed topography and distribution of manganese nodules in the Central Indian Ocean. *Mahasagar*: 21:7-12.
- Piper, D. Z., and M. E. Williamson. 1977. Composition of Pacific Ocean ferromanganese nodules and its relationship to sediment accumulation rates. *Mar. Geol.* 23:285-303.
- Price, N. B., and S. E. Calvert. 1970. Compositional variation in the Pacific Ocean ferromanganese nodules and its relationship to sediment accumulation rates. *Mar. Geol.* 9:145-177.
- Raab, W. 1972. Physical and chemical features of Pacific deep sea manganese nodules and their implications to the genesis of nodules. In *Ferromanganese deposits of the ocean floor*, D. R. Horn, ed. Washington, DC: National Science Foundation, pp. 31-49.

- Siddiquie, H. N., N. H. Hashimi, A. R. Gujar, and A. B. Valsangkar. 1984. Superficial mineral resources of the Indian Ocean. *Deep-Sea Res.* 31:763-812.
- Sorem, R. K., R. H. Fewkes, W. D. McFarland, and W. R. Reinhart. 1979. Physical aspects of growth environment of manganese nodules in the "HORN Region", east equatorial Pacific Ocean. In *La genese des nodules de manganese, September, 1978*, C. Lalou, ed. Colloques internationaux du Centre de la Recherche Scientifique, CNRS, vol. 289, pp. 61-76.
- Sudhakar, M. 1988. Relation between grade and abundance of manganese nodules. *Current Sci.* 57:662.
- Udinstev, G. B., ed. 1975. *Geological and geophysical atlas of the Indian Ocean*. Moscow: Academy of Sciences of USSR, p. 23.
- Usui, A. 1979. Minerals, metal contents and mechanism of formation of manganese nodules from the Central Pacific Basin (GH 76-1 and GH 77-1 areas). In *Marine geology and oceanography of the Pacific manganese nodule province*, J. L. Bischoff and D. Z. Piper, eds. New York: Plenum, pp. 651-680.
- Valsangkar, A. B., G. V. Rajamanickam, S. M. Karisiddaiah, and H. N. Siddiquie. 1988. Morphological and inter layer geochemical studies on manganese nodules from the southwestern Carlsberg Ridge. *Mar. Geol.* 84:81-94.